Desalination and Water Treatment
www.deswater.com

doi: 10.5004/dwt.2017.21268

87 (2017) 1–13
August

Effects of concentrator type and encapsulated phase change material on the performance of different solar stills: an experimental approach

T. Arunkumar[a,*], R. Velraj[a], Gustavo Otero Prado[b], D.C. Denkenberger[c], Omid Mahian[d], R. Sathyamurthy[e], K. Vinothkumar[f], A. Ahsan[g]

[a]*Institute for Energy Studies, Anna University, Chennai – 600025, Tamilnadu, India, email: tarunkumarsolar@gmail.com (T. Arunkumar), velrajr@gmail.com (R. Velraj)*
[b]*Institute of Technology and Exact Sciences, Federal University of Triângulo Mineiro, Uberaba, MG, Brazil, email: webgop@yahoo.com.br*
[c]*Department of Civil and Architectural Engineering, Tennessee State University, Nashville, TN, USA, email: david.denkenberger@gmail.com*
[d]*Mechanical Engineering Department, Engineering Faculty, Ferdowsi University of Mashhad, Mashhad, Iran*
[e]*Department of Mechanical Engineering, S.A. College of Engineering, Chennai, Tamilnadu, India, email: raviannauniv23@gmail.com*
[f]*CHOGEN Powers Pvt. Ltd., Chennai, Tamilnadu, India, email: vinoy2kenergy@rediffmail.com*
[g]*Department of Civil Engineering, Institute of Advanced Technology, University Putra Malaysia, 43400 UPM Serdang, Selangor, Malaysia, email: ashikcivil@yahoo.com*

Received 13 February 2017; Accepted 29 July 2017

ABSTRACT

An experiment has been performed to study the effect of system integration by two different concentrator assisted de-salting systems. The compound parabolic concentrator (CPC) and compound conical concentrator (CCC) are used in this research work. Two solar desalination systems, the single slope solar still (SSSS), and pyramid solar still (PSS), have been integrated with a CCC and compound parabolic concentrator-concentric circular tubular solar still (CPC-CCTSS). To study the effect of system integration, a thick cloth prevents the entry of sunlight into the solar still top. Additionally the concentrator assisted de-salting systems are equipped with phase change material (PCM) for enhancement. In CCC-SSSS, the PCM fills the inside of hollow copper balls and the balls are placed in the SSSS basin. In the CPC-CCTSS, the PCM is loaded in the specially designed circular trough. Two methodologies are followed here to produce the fresh water even while the distillers are blocked from the sunlight. They are (1) thermosyphon effect in CCC-SSSS and (2) waste heat recovery from CPC-CCTSS. The results showed that the productivity of CCC-SSSS, CCC-SSSS with PCM, and CCC-SSSS (PCM) top cover shaded were found as 2680 mL/m^2/d, 3240 mL/m^2/d and 1646 mL/m^2/d, respectively. Similarly the productivity of the CPC-CCTSS-PSS, CPC-CCTSS (PCM)-PSS and CPC-CCTSS (PCM)-PSS top cover shaded were found as 7160 mL/m^2/d, 7346 mL/m^2/d, and 5120 mL/m^2/d. The productivity of the CCC-SSSS and CPC-CCTSS-PSS is examined and conclusions are drawn such as the solar radiation blocked distillers productivity did not drop to zero.

Keywords: Compound conical concentrator; Compound parabolic concentrator; Desalination; Pyramid solar still; System integration

1. Introduction

"*The duties of life cannot be discharged by any person without water, so without rain there cannot be the flowing in water*" says *Thirukural*, written by the saint *Thiruvalluvar* approximately 2,200 years ago in Tamil Nadu [1]. This passage clearly indicates the importance of water and is well matched with the present situation. Nowadays, the need of fresh water is greater due to the remarkable growth of population. It is very hard to predict the available fresh water for the next 50 years. A solar still is a device which can convert available waste or brackish water into potable water using solar energy [2,3]. Solar stills are very well studied over the last

*Corresponding author.

30 y by scientists worldwide [4,5]. This technology is conceptually old but effective for the present and future scenario. To consider the future requirements, researchers seek new solutions to produce fresh water in sustainable ways.

System integration plays an important role to enhance the performance of solar distillers. Basically, the solar stills are known as units with low productivity. The basin of the solar still absorbs the energy only from the Sun. Additional heat supplied in a sustainable way is required to augment the evaporation process in solar stills [6]. Nowadays, solar concentrators are identified as a heat source unit for coupled systems. Concentrator powered solar distillation systems play a significant role in producing fresh water. Presently researchers are involved in these activities to accumulate high-quality de-salted water through innovative methodologies like wind-powered desalination [7] and nano-composite energy storage [8,9].

Dev et al. [10] experimentally studied an inverted solar still and conventional solar still at different water depth. The result shows that a higher temperature is observed in an inverted absorber solar still than in a conventional one. Xie et al. [11] experimentally studied the low-temperature multi-effect desalination (LT-MED) system. Estahbanti et al. [12] experimentally tested the internal reflector on the productivity of a conventional solar still during the summer and winter. The internal reflectors are pasted on the side walls of the solar still. The result shows that the solar still with internal reflectors on the front and side walls enhanced the system efficiency by 18%.

Gorjian et al. [13] designed a parabolic point focus solar still. The experimental device consists of a two axis sun tracker, parabolic dish concentrator and heat exchanger. The maximum productivity of 5.12 kg within 7 h was measured and the daily efficiency is 36.7%. Omara and Eltawil [14] designed and developed a solar dish concentrator (SDC) for brackish water desalination. A mini single slope solar still was designed and installed at the focus of the dish concentrator. The results concluded that the daily average distillate water was 6.7 L/m^2/d and the corresponding efficiency is 68%.

Arunkumar et al. [15] experimentally studied the tubular solar still (TSS) with a rectangular absorber for water desalination. Air or cooling water was passed through the concentric tubular solar still to extract the waste heat from the TSS. The results were that the cooling water embodiment gave the maximum productivity of 5 L/m^2/d, greater than with the air flow. Concentration of solar radiation is attained using a reflecting arrangement of mirrors or lenses. In the past few years, significant advancement have been made in the development of concentrating collectors [16–19]. Concentrators are one of the best tools to integrate with solar distillation system to improve the evaporation rate. Many authors have performed the distillation process with various solar concentration techniques [20–33].

Thermal energy storage (TES) is an environmentally friendly technology that helps to economically bridge the gap between the energy supply and end-user demand. The concept of energy storage is very important in many industrial and commercial applications. However, this technology has received greater attention only in recent years because of the growth of renewable energy, particularly in the field of solar energy. In a TES system, heat can be stored in a sensible/latent heat form or by thermochemical reactions. In sensible thermal storage (STS), heat energy is stored by increasing the temperature of the solid/liquid storage medium. Latent heat storage stores the heat in a phase change material (PCM). Compared with sensible heat storage, latent heat storage density is much higher. The research on PCM is popular because of this [34].

El-Sebaii et al. [35] studied a single slope solar still with stearic acid as a PCM. A computer simulation was also used to investigate the performance of the solar still. The stearic acid was put in the basin liner with thickness 0.2 cm. They concluded that distillate productivity (9.005 kg/m^2/d) with a daily efficiency of 85.3% was obtained compared to 4.998 kg kg/m^2/d when the still is used without PCM.

Naim and Kawi [36] studied paraffin wax with sodium chloride solution as a PCM in a solar still. About 70 ml of aqueous sodium chloride solution with paraffin was placed beneath the solar still at 0.5 cm gap thickness. The results showed that the PCM increases the productivity of the solar still significantly. Radhwan [37] conducted an experimental work in a stepped solar still with paraffin wax that acts as a PCM. The proposed system was designed with five stepped basins and an inclined glass cover. The results showed that the stepped solar still with a PCM has an efficiency of 57% and the productivity is 4.6 L/m^2. Arunkumar et al. [38] experimentally studied a concentrator assisted solar still with PCM. It was found that the productivity of the system was improved by 26% because of the influence of the PCM.

A modified solar still using hot air injection and PCM was experimentally studied by Kabeel et al. [39]. 17.5 g of paraffin wax was used in the basin. The results showed that the PCM integrated hot air injection modified solar still productivity is 9.36 L/m^2/d and 4.5 L/m^2/d for conventional solar still. Kabeel and Abdelgaied [40] performed experiments in a solar still with paraffin wax as a PCM. Two identical solar stills were constructed with an area of 0.615 m^2. 17.5 g of paraffin wax was used in this study. The daily fresh water productivity was measured for solar stills with PCM as 7.54 L/m^2, and without PCM as 4.51 L/m^2. The PCM enhanced the overall productivity by 60%. Dashtban and Tabrizi [41] conducted an experiment in a weir type cascade solar still with paraffin wax as the PCM. 18 g of paraffin wax was used beneath the solar still to store the thermal energy. The results showed that the PCM enhanced the productivity by 31%. Chaichan and Kazem [42] studied a solar distiller using a concentrating solar water heater and PCM. The paraffin wax was selected as the PCM and it was placed beneath the basin liner. The results showed that proper solar tracking with a PCM in the distiller improved the system productivity by 307%.

Sathyamurthy et al. [43] experimentally studied a triangular solar still with paraffin wax as a PCM. From the experimental results, the paraffin wax enhanced the productivity by 35% as compared with a conventional solar still. Also, the productivity of with and without PCM in the triangular solar stills was 5.5 L/m^2 d and 3.5 L/m^2 d, respectively.

Based on the literature review, all the modifications have been focused towards system integration to increase the fresh water production. In this present work, solar stills are equipped with a CCC or CPC. This study is a real-time analysis of the impact of system integration. Here, a CPC-CCTSS is designed and integrated with a PSS (CPC-CCTSS-PSS). In the same way, a CCC is coupled with SSSS (CCC-SSSS). In the continuation of the experimental study, the PCM is also added to the SSSS and CCTSS. The top covers of the solar stills are artificially covered by a cloth to block the sun light and to study the effect of integration by the concentrator on the solar desalination system.

2. Materials

2.1. Solar radiation measuring instruments and other devices

The geographical information on the experimental location is shown in Fig. 1. The solar radiation measuring instruments are illustrated in Fig. 2A pyranometer (accuracy ± 30 W/m^2, range 0–1750 W/m^2) is used to measure the solar irradiance. A digital thermometer (accuracy ± 1°C, range 0–100°C) and K-type thermocouples (accuracy ± 1°C, range 0–100°C) are used to assess the temperature of CPC-CCTSS-PSS and CCC-SSSS. A digital hygrometer (± 0.5°C ± 1%, range 10–99%) is used to monitor the humidity during the experimentation [44–47].

2.2. Details of CCC-SSSS

Figs. 3, 4 show the schematic diagram of a CCC-SSSS and CCC-SSSS with PCM. The basin dimensions are 0.5 m × 0.5 m and it is composed of galvanized iron sheet coated with black paint. The outer box is made of wood with dimensions of length (0.7 m), breadth (0.7 m) and thickness (0.004 m). In the SSSS, saline water is allowed to fill up to 3 cm in the basin. To reduce the heat losses from the solar still, saw dust is used at the bottom and side walls. These insulation layers reduce the conduction heat loss through the base and sides of the solar still [32]. Clear glass with a transmissivity and thickness of 0.88 and 4 mm, respectively, is used as the cover material. Grooves are provided at all the edges of the solar still so that the cover is rigidly supported. An inclination of 11° is provided to the glass cover so that the condensed droplets glide down to the distillate collector provided at the end of the cover. The PCM is loaded with the help of copper balls (see Fig. 5). The diameter of the copper balls is 28 mm and they are painted black. These balls have a small hole on their tops and the paraffin wax is filled through the hole and sealed with a rubber cork. These copper balls are filled with 25 g of paraffin wax uniformly. The positions of the rubber cork in the copper balls are properly monitored each day before the commencement of experiment. The temperatures of the PCM loaded copper balls are measured by K-type thermocouples.

The water circulates from the still and the absorber through the pipe under thermosyphon effect. The concentrator is adjusted manually to track the sun. The pipes carrying the water are insulated for the sake of minimum conduction loss of heat to the ambient during water circulation. The reflected radiation from the CCC incident on

Fig. 2. Solar radiation measuring instruments.

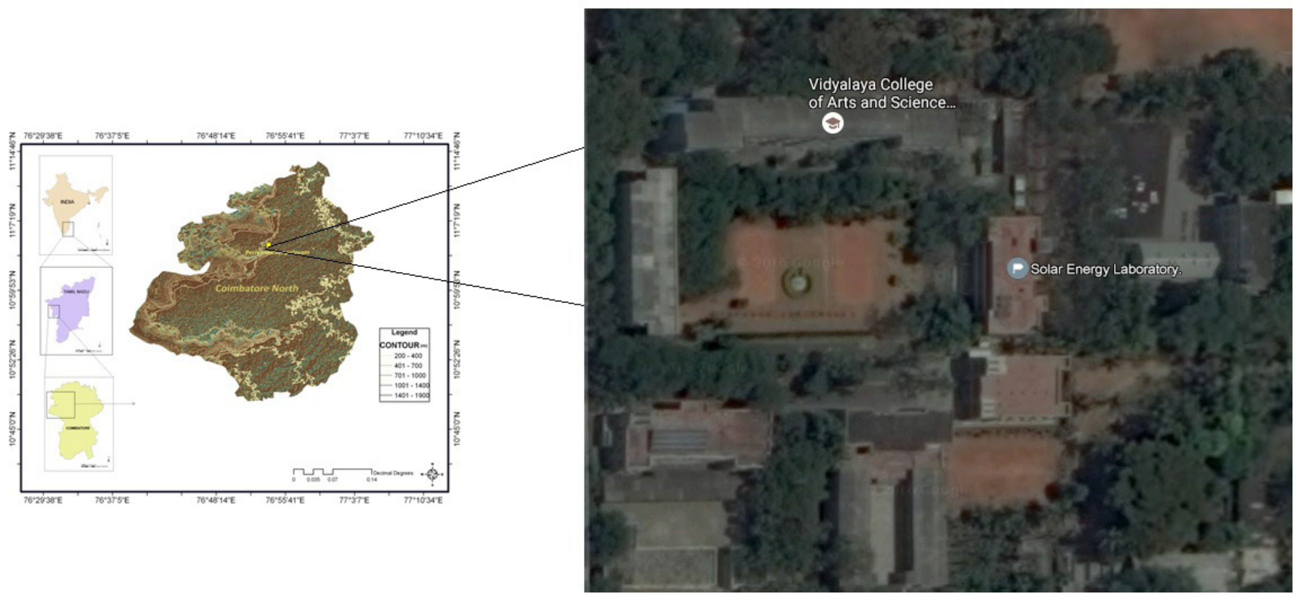

Fig. 1. Geographical information of the experimental location.

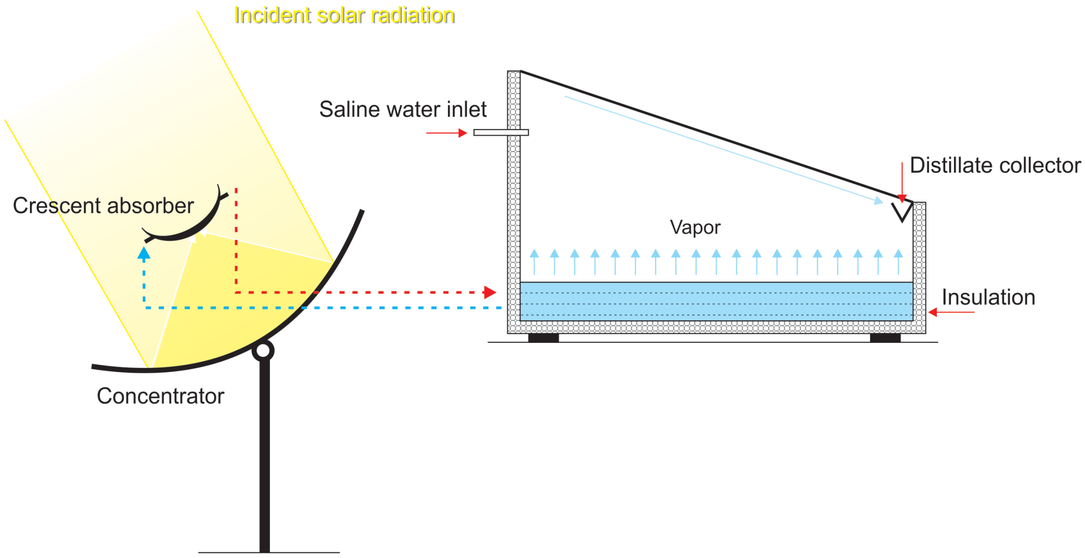

Fig. 3. Schematic view of CCC-SSSS.

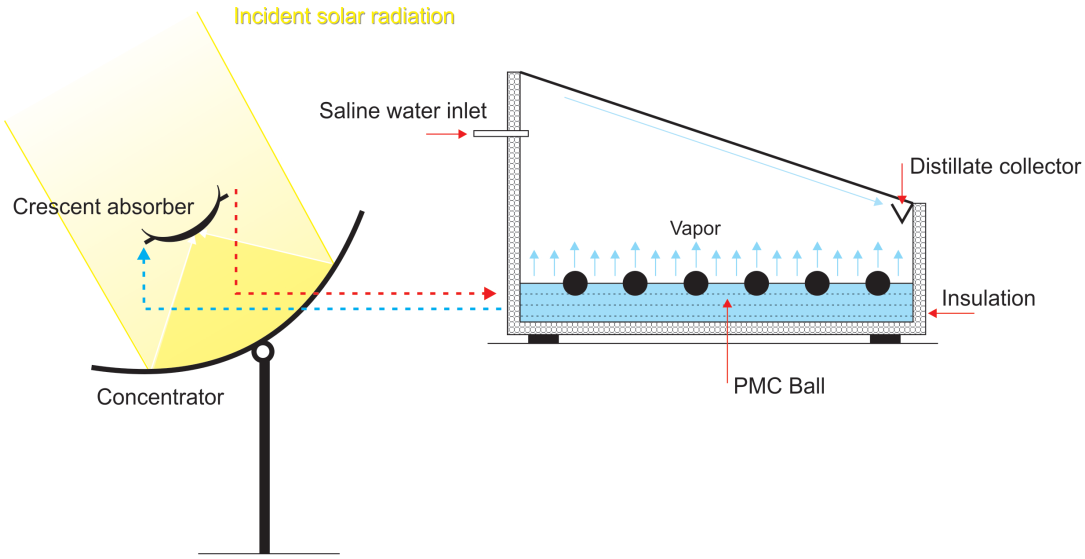

Fig. 4. Schematic view of CCC-SSSS with PCM.

Fig. 5. The PCM loaded copper balls with rubber cork.

the crescent absorber heats the water. The hot water being less dense rises and enters the solar still. Then colder water from the solar still follows. The water in the basin is heated by the solar radiation and the circulation of hot water from the crescent. Therefore, the water in the basin gets heated and evaporates moisture into the air trapped between the water surface and the glass cover. The evaporated water condenses under the glass cover and is collected by the distillate collector.

2.3 Arrangement of CCC-SSSS with crescent shaped absorber

The CCC (focal length 0.40 m, thickness 0.5 mm, net weight 6.2 kg) of diameter 1 m is used in this study. Aluminum foil is pasted on the CCC for good reflection. The CCC coupled crescent shaped absorber is connected with the SSSS. The pictorial view of crescent shaped absorber is shown in Fig. 6. The designed shape like a crescent moon is to collect all the reflected radiation from the CCC and be aesthetically attractive. Since it is made of copper, this helps to smooth out any temperature differences due to imperfect concentration. This crescent absorber is placed at the focus of the collector to convert the solar energy to heat, which increases the water temperature. The absorber is made up of copper (hollow) of thickness 3 mm. The diameter of the crescent absorber is 0.26 m and the height is 0.07 m. Two 13 mm pipes are connected with both the ends of the absorber, which act as inlet and outlet. This inlet and outlet were coupled with the SSSS. The bottom of the basin still is connected to the inlet of the crescent absorber. The outlet of the crescent absorber is again connected with water in the basin. Heat energy circulated between water in the basin and the crescent absorber is due to the thermosyphon effect. A spherical shape of the crescent absorber is maintained at the bottom to receive solar radiation focused by the concentrator (aperture area 0.785 m^2) (D = 1 m, and S = $pD^2/4$ = 0.785 m^2). The side view of the CCC-SSSS is shown in Fig. 7. Pictorial views of CCC-SSSS with and without top cover shading are shown in Fig. 8.

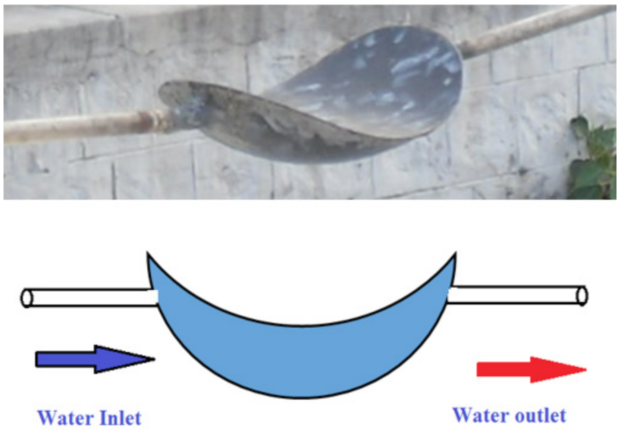

Fig. 6. Pictorial and schematic view of crescent shaped absorber.

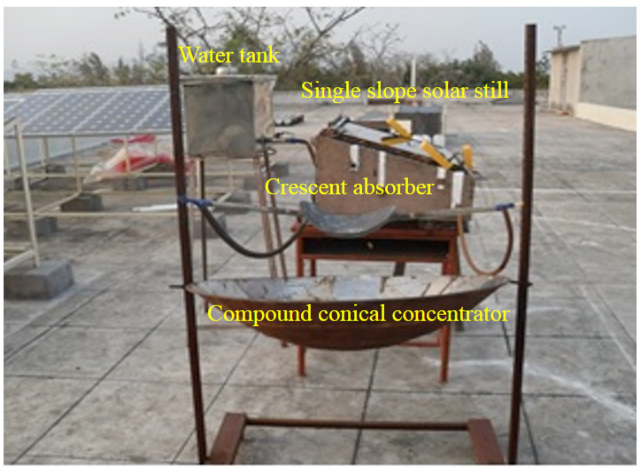

Fig. 7. Side view of the CCC-SSSS and complete view of the solar energy laboratory.

3. Design of the CPC [48]

The reflector profile for the CPC with a 'V' groove at the bottom is such that all rays entering the cavity end up at the absorber. It can be drawn for a tubular absorber of radius r_1, and half acceptance angle θ_A allowing a small space δ between cavity opening and the absorber (Fig. 9).

$$x = r_1 \sin\theta - \rho\cos\theta \tag{1}$$

The upper portion of the reflector profile AB and CD can be generated using the relation,

$$x = -r_1 \cos\theta - \rho\sin\theta \tag{2}$$

where ρ is the ground reflectance

$$\rho = r_1\left[\theta + \Delta\theta\right] \tag{3}$$

For the angles

$$\pi - (2\varphi + \varepsilon) \le \theta \le \theta_A + \pi/2$$
$$\rho = \frac{r_1[\theta + \theta_A + \pi/2 + 2\Delta\theta - \cos(\theta - \theta_A)]}{[1 + \sin(\theta - \theta_A)]} \tag{4}$$

Fig. 8. Pictorial view of CCC-SSSS with two modes of operation.

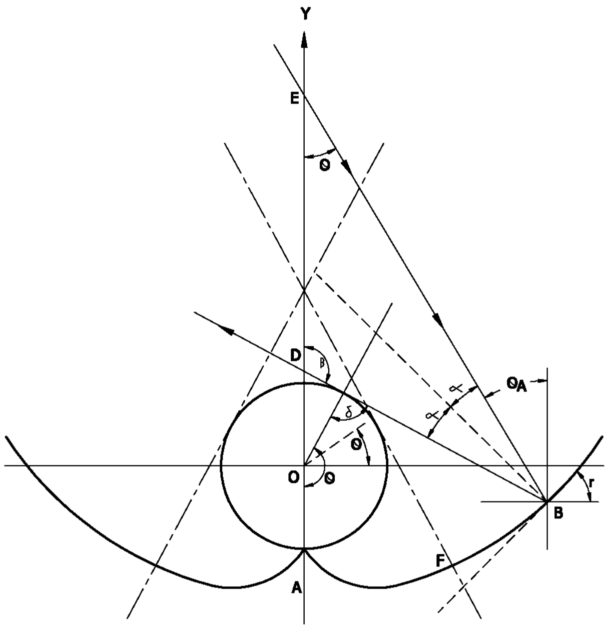

Fig. 9. Reflector shape for tubular absorber.

For the range of angles

$$\pi / 2 + \theta_A \leq \theta \leq 3\pi / 2 - \theta_A$$

where

$$\Delta\theta = \cot\varphi - \left[\pi - (2\phi + \varepsilon)\right] \tag{5}$$

And from Fig. 1,

$$\phi = \sin^{-1}(r_1 / r_2) \tag{6}$$

$$\phi + \varepsilon = \sin^{-1}[(r_1 + \delta) / r_2] \tag{7}$$

The upper portion of the radius of envelope is

$$r_2 = \frac{[r_1^{\,2} + (\delta / 2\sin\alpha)^2 + \delta r_1]^{1/2}}{\cos\alpha} \tag{8}$$

$$(1 / \sin\alpha) - \sin\alpha = \delta / 2r_1 \tag{9}$$

The bottom region of the profile can be modified by incorporating a V-shaped reflector portion just below the absorber.

The height 'h' and the open angle '2Ψ' of the 'V' groove are related by the following relations

$$\pi - 2\alpha \leq 2\psi \leq \pi / 2 + \alpha \tag{10}$$

$$\sin\alpha = r_1 / (r + \delta + h) \tag{11}$$

Average fraction of radiation lost 'L' is given by

$$L \approx \frac{\varepsilon^2}{2(1 + 2\phi\tan\phi)} \tag{12}$$

And the ratio of the concentration achieved to the maximum possible concentration of the concentrator is calculated as

$$\frac{CR}{CR_{\max}} = \frac{\cot\phi + 2\phi + \varepsilon}{\pi} \tag{13}$$

where

$$CR_{\max} = 1 / \sin\theta_A \tag{14}$$

3.1. Details of CPC-CCTSS-PSS

The circular shaped trough is used to store the saline water (see Fig. 10). The specifications of the CPC-CCTSS are given in our previous work [15]. The inner and outer circular tubes (concentric) are positioned with a 5 mm gap for the flowing water and air to cool the outer surface of the inner tube. Paraffin wax (melting point 58–60°C, latent heat of fusion 226 kJ/kg, solid density 818 kg/m^3, thermal conductivity 0.24 W/m°C and specific heat 2.95 kJ/kg°C) is used as the PCM in this research work. The PCM is loaded in a specially designed portion of the absorber which is located at the bottom of the circular water storage trough. The circular storage trough is made up of copper. Two circular shaped basins are joined with a gap of 5 mm for loading the PCM, which is shown in Fig. 11. The PCM is loaded to a desired quantity and at the same time to not burst despite high temperatures. The absorbers for the system are modified to introduce the storage effect with the help of the PCM. A good quality circular strip was fabricated by a machine and two small pieces of the same material were welded properly in the front and back sides. A storage tank mounted on a steel structure supplied raw water and cooling water. The heated water from the CPC-CCTSS is allowed to fill the PSS basin up to a depth of 3 cm. The cooling water exit was connected to the PSS. The inclination angle from the horizontal of the PSS glass cover was 48.9°. Fig. 12 illustrates the overall view of CPC-CCTSS-PSS.

3.2. Arrangement of CPC-CCTSS-PSS

Five CCTSS and the same number of saline water storage circular shaped troughs were fabricated. The water storage troughs were carefully placed inside the concentric tubular cover and proper leveling was ensured. The optimum level of saline water was filled inside the trough using a burette and blocked the all the sides without any air gap. The CCTSS is carefully placed over the focal point of the CPC [31] for experimentation. The thermocouples are adjusted and fixed at the appropriate places to measure the temperature profile of the CPC-CCTSS. The CPC-CCTSS-PSS and CPC-CCTSS-PSS top cover shaded views are shown in Fig. 13. The distillate collector is used to collect the output from the CCTSS.

Fig. 10. Circular water storage trough with PCM.

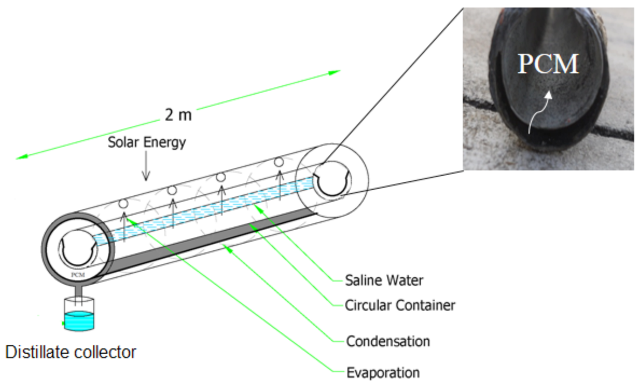

Fig. 11. View of CCTSS with PCM portion.

4. Heat transfer mechanism of solar still with crescent shaped absorber

The internal heat transfer occurs within the solar still from the water surface to the inner glass cover, which mainly consists of evaporation, convection and radiation. The convective and evaporative heat transfers take place simultaneously and are independent of the radiative heat transfer. Convective heat transfer (natural convection) takes place across the humid air inside the SSSS basin due to the temperature difference between the water and the inner glass cover. Also the temperature difference between the hot surface of the crescent absorber and the fluid inside the absorber causes density reduction in the fluid above the surface, resulting in buoyancy. The circulating water gained heat energy from the external absorber and the heat is lost inside the SSSS to enhance the desalination process.

5. Results and discussion

The present experiments were performed under Coimbatore (11°N, 77°E), India climatic condition during January 2012 to November 2012. Fig. 14 shows variation of solar irradiance with respect to time of day. The average received solar insolation for CCC-SSSS, CCC-SSSS (PCM) and CCC-SSSS top cover shaded are 827 W/m^2, 856 W/m^2 and 846 W/m^2. Similarly the average received solar radiation corresponds to CPC-CCTSS-PSS, CPC-CCTSS (PCM)-PSS and CPC-CCTSS (PCM)-PSS top cover shaded are 873 W/m^2, 867 W/m^2 and 832 W/m^2. This experiment is done with a single distiller unit subjected to different climatic conditions. The difference in insolation for the different configurations is only a few percent, and therefore the larger variations in output are statistically significant. The recorded ambient temperature is shown in Fig. 15. Ambient temperature

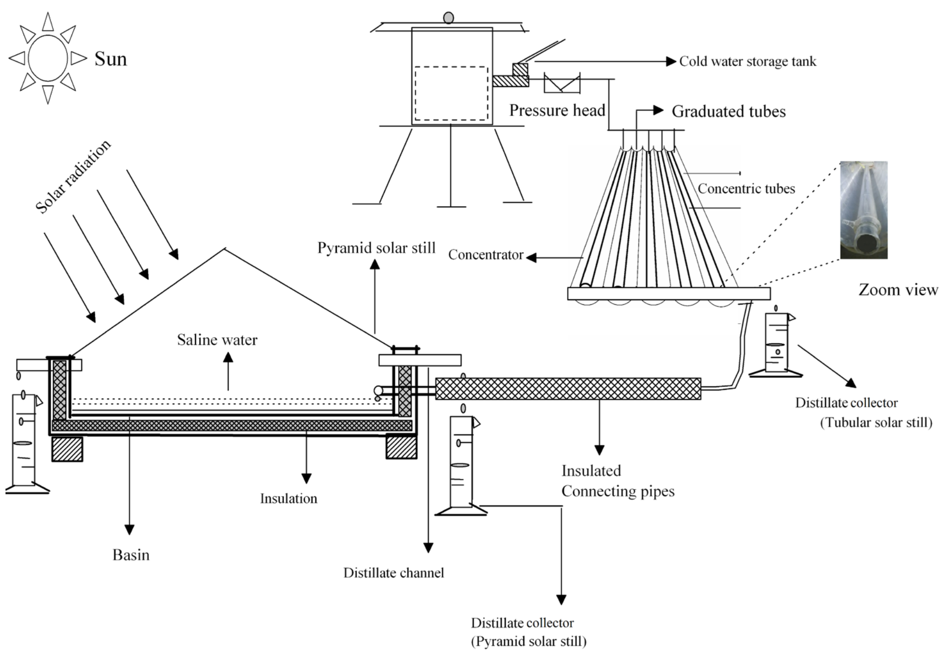

Fig. 12. Schematic view of CPC-CCTSS-PSS.

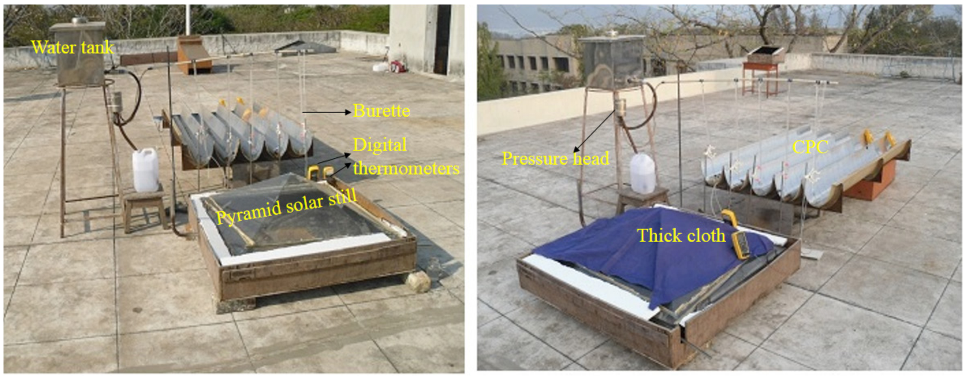

Fig. 13. CPC-CCTSS (PCM)-PSS with two modes of operation.

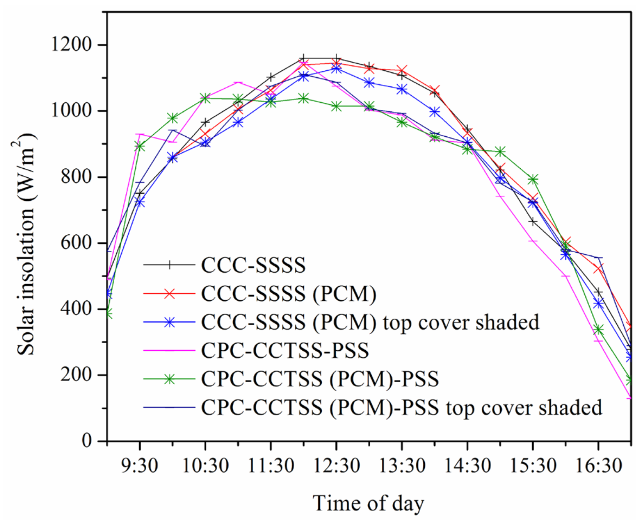

Fig. 14. Solar insolation with respect to time.

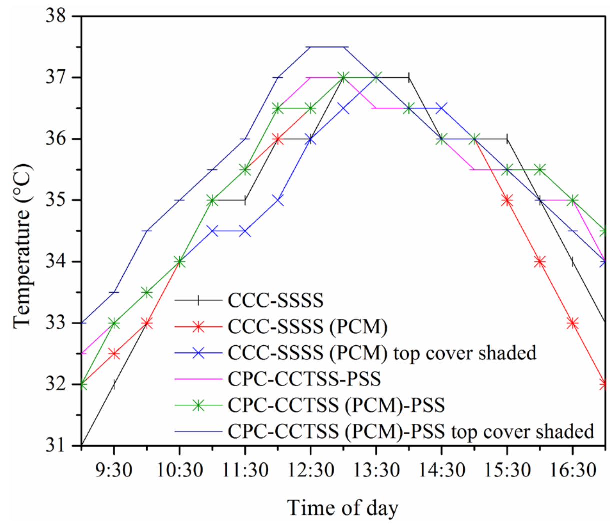

Fig. 15. Ambient temperature with respect to time.

variations play an important role in the overall productivity of the solar distiller. The recorded wind condition during the experiment is 1.2 m/s. Wind is one of the important parameters that increases the natural circulation inside the solar still. The productivity increases with increase of wind velocity. The wind decreases the top glass temperature. So the temperature difference between the glass and water in the basin is increased, which causes an increase in distillate productivity.

Figs. 16a, b show the variation of water temperature (T_w), air temperature (T_{air}) and outer cover temperature (T_{oc}) with respect to time for the SSSS and top cover shaded SSSS. The SSSS (Fig. 16a) maximum of T_w, T_{air}, and T_{oc} are measured as 68°C, 61°C and 45°C. Similarly the top cover shaded SSSS (Fig. 16b) maximum of T_w, T_{air}, and T_{oc} are measured as 61°C, 50°C and 39°C. It is observed from these results that the water temperature is decreased 7°C by the shading effect. The temperature inside the SSSS is not much affected by the shading effect on SSSS due to the continuous entry of hot water from the crescent shaped absorber. Fig. 17 shows the variation of water temperature (T_w), air temperature (T_{air}) and outer cover temperature (T_{oc}) with respect to time for the CCC-SSSS (PCM). The maximum of T_w, T_{air}, and T_{oc} are measured as 71°C, 59°C and 44°C. Fig. 18 shows the temperature of the crescent shaped absorber connected with CCC-SSSS. Here, the PCM melts between 58–60°C, absorbing heat; when it changes to a solid form, it releases this heat. This phase change is used for storing heat in PCMs. The graphical representation concludes that the water temperature slightly increased at 16:30 due to the PCM releasing the heat to its surroundings. The encapsulated PCM is identified as a most promising candidate to store the thermal energy. The maximum recorded temperature in the crescent shaped absorber is 93°C. The crescent shaped absorber gets heated by the incoming solar radiation and reflected flux from the CCC.

The inlet and outlet water temperatures of the CCC-SSSS are given in Fig. 19. The maximum temperature recorded at the inlet location (measured between the SSSS and the crescent absorber) was 62°C and the outlet temperature (between the crescent absorber and the SSSS) was 89°C. The water in the basin is heated by the circulation of hot water even when the top cover is shaded. Therefore, the productivity does not drop to zero. The purpose of the cotton cloth used here is to find the concentrator's effect by shading the top cover. The productivity is very significantly

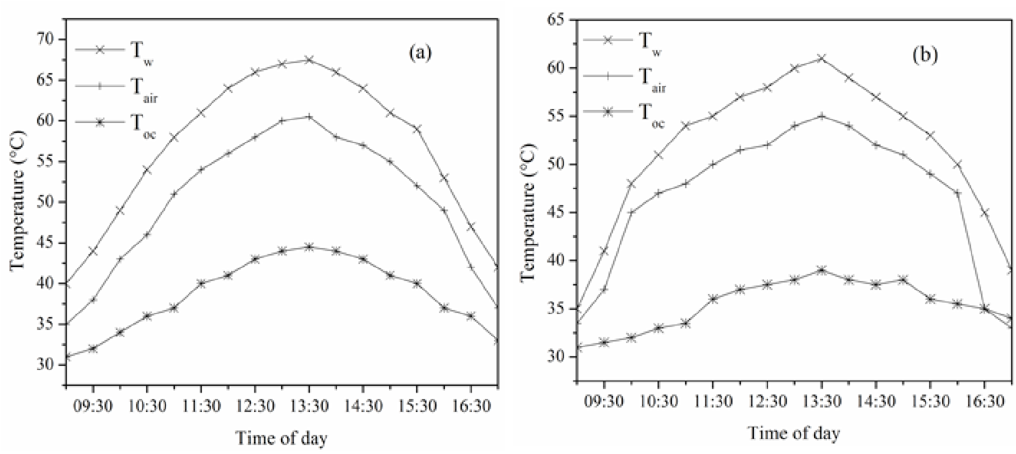

Fig. 16. (a) Hourly variation of temperature in SSSS, (b) SSSS top cover shaded.

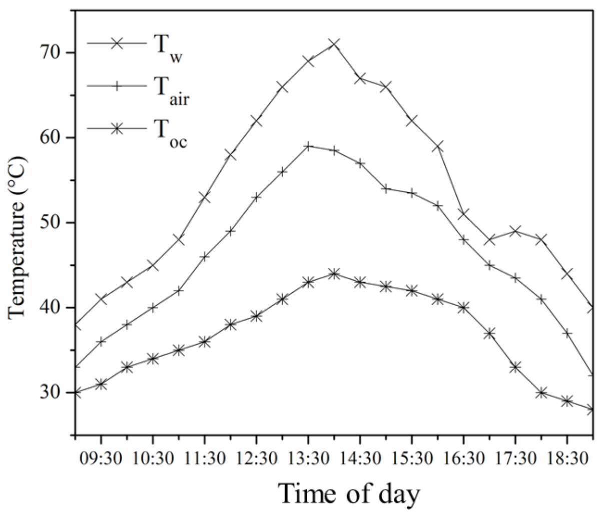

Fig. 17. CCC-SSSS with PCM.

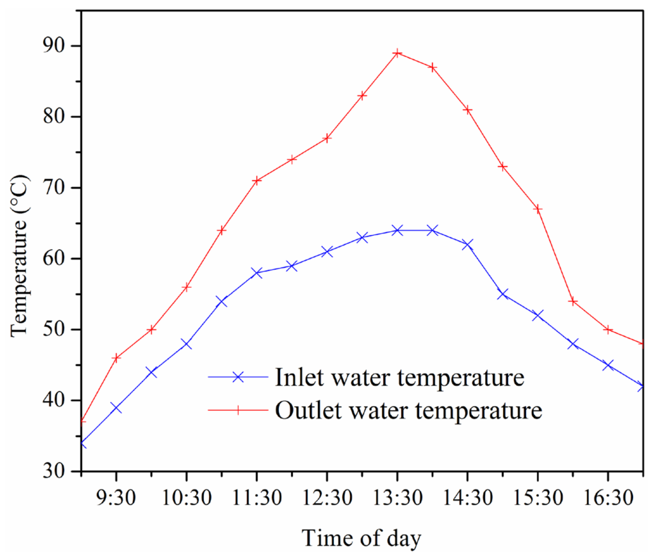

Fig. 19. CCC-SSSS inlet and outlet temperature.

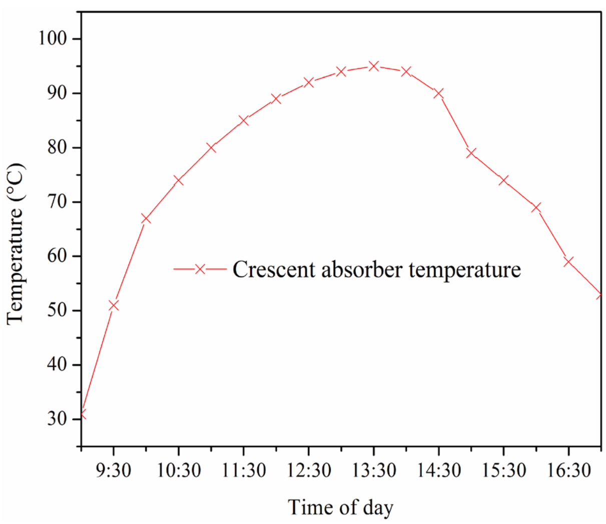

Fig. 18. Temperature of crescent shaped absorber used in the CCC-SSSS.

affected due to the solar still being covered by the cotton cloth. So natural circulation of hot water to solar still from crescent shaped absorber has been verified experimentally.

Fig. 20 shows the CPC-CCTSS temperature with respect to time. The maximum measured water, air and outer cover temperatures are 94°C, 68°C and 50°C, respectively. The recorded results showed that the CPC-CCTSS acts as a heat source for the PSS. Fig. 21a,b shows the variation of water, air and outer cover temperatures with respect to time for the PSS and top cover shaded PSS. The PSS maximum temperatures of T_w, T_{air}, and T_{oc} are measured as 68°C, 59°C and 44°C, respectively. Similarly the top cover shaded maxima of T_w, T_{air}, and T_{oc} are measured as 60°C, 49°C and 36°C, respectively. It is observed from the results that the water temperature was decreased 8°C by the shading effect. This relatively small effect on the temperature is despite shading of the PSS is due to the continuous entry of hot water from the CPC-CCTSS. The heat extracted water temperature coming from the CPC-CCTSS is roughly the operating temperature for the PSS. The K-type thermocouple is fixed between the two layers of the circular trough and welded with a circular strip. Fig. 22 shows the variation of T_w, T_{air} and T_{oc} with respect to time for the CPC-CCTSS (PCM). The maximum of T_w, T_{air}, and T_{oc} are measured as 92°C, 70°C and 64°C, respectively.

Fig. 23 shows the inlet and outlet temperature of CPC-CCTSS-PSS. The maximum recorded inlet temperature (measured between ambient water to CCTSS) is 41°C and outlet temperature 70°C. The cold water (from the water tank) flow is highly beneficial because the water in the trough (CCTSS) approaches the boiling point. The inlet temperature is measured between the water tank and the entry of the first CCTSS and the outlet temperature is measured between the CPC-CCTSS and the PSS. A storage tank is used to pass the water at 10 mL/min with the help of burette. The CCTSS water storage trough attained maximum temperature early. At the same time the inner tube temperature was also high due to (1) the trough and top cover being separated by a small distance, and (2) the reflected flux from CPC. This large temperature causes steam generation instead of fresh water condensation. Then, ambient water from the storage tank is allowed to pass though the CCTSS inlet portion. The flow water is adjusted to 10 mL/min to extract the heat from the top cover of the inner tube (see Fig. 10). The heat extraction at the CPC-CCTSS induced a larger temperature difference between the condensing cover and the water storage trough. Heat extracted by CPC-CCTSS was successfully delivered to the PSS and this heat supply caused a larger evaporative heat transfer. The direct link system reduces the warm-up time of the PSS. The salient feature is that the flow of water induced a larger ΔT in the CPC-CCTSS and PSS at the same time. This process repeats in every cycle and enhances the fresh water production.

Fig. 24 shows the fresh water productivity with system integration. The results are that the productivity of CCC-SSSS, CCC-SSSS (PCM), and CCC-SSSS (PCM) top

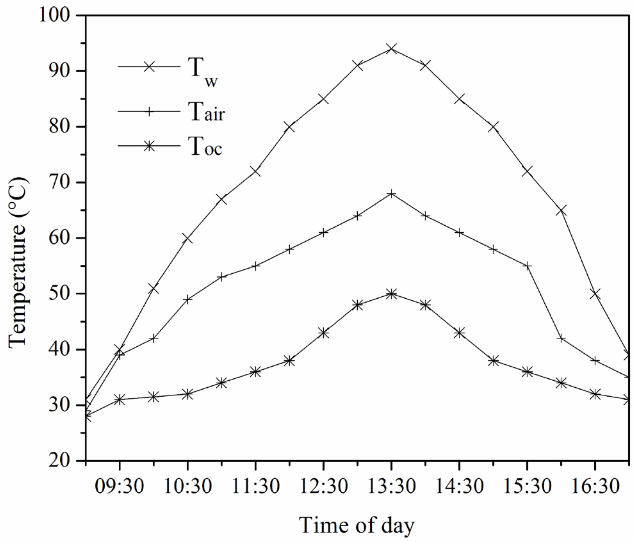

Fig. 20. Hourly variation of CPC-CCTSS temperature profile.

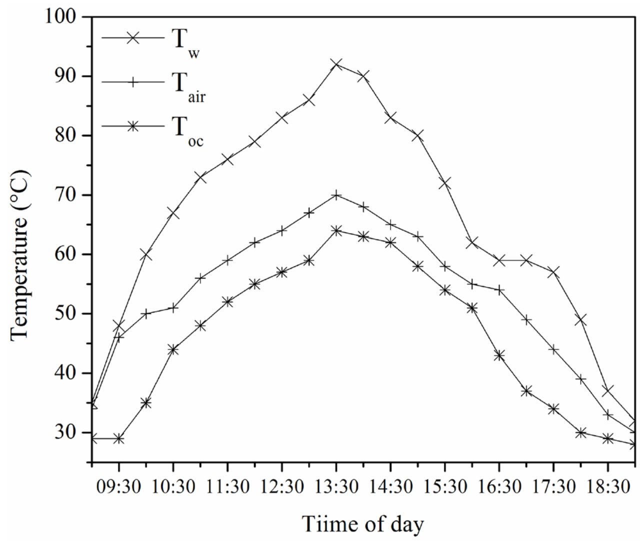

Fig. 22. CPC-CCTSS with PCM.

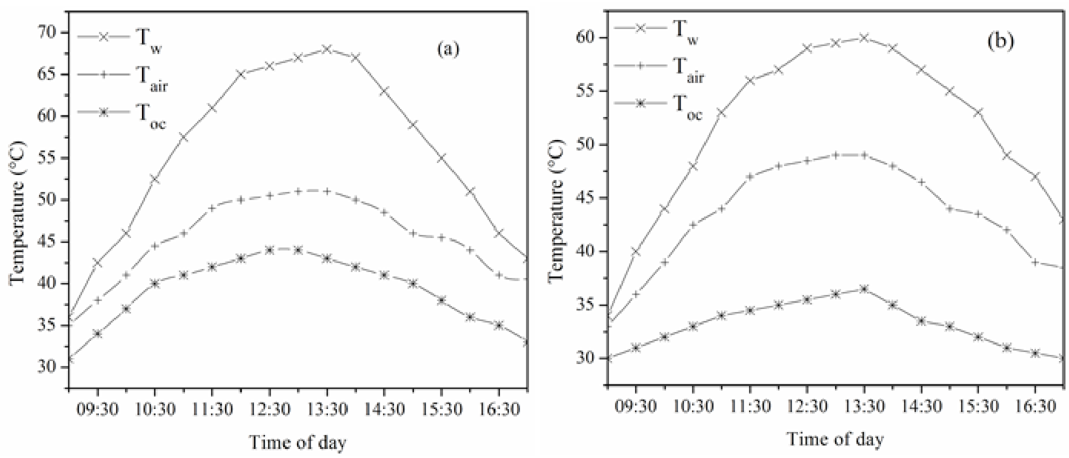

Fig. 21. (a) Hourly variation of temperature in PSS, (b) PSS top cover shaded.

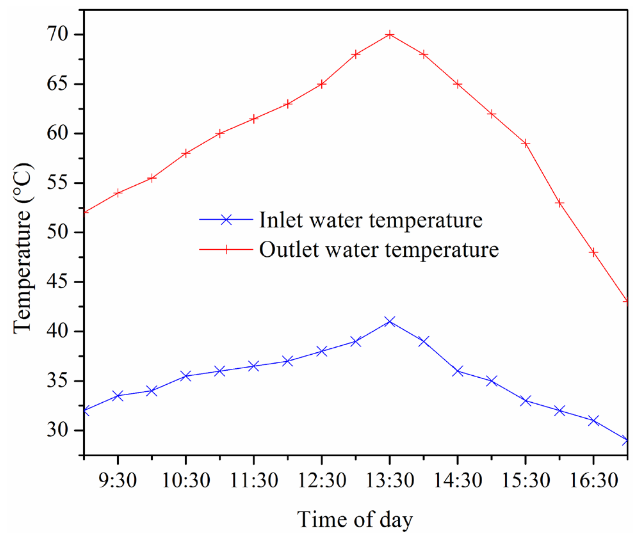

Fig. 23. Inlet (between water tank and CCTSS) and outlet (between CCTSS and PSS) temperature of CPC-CCTSS.

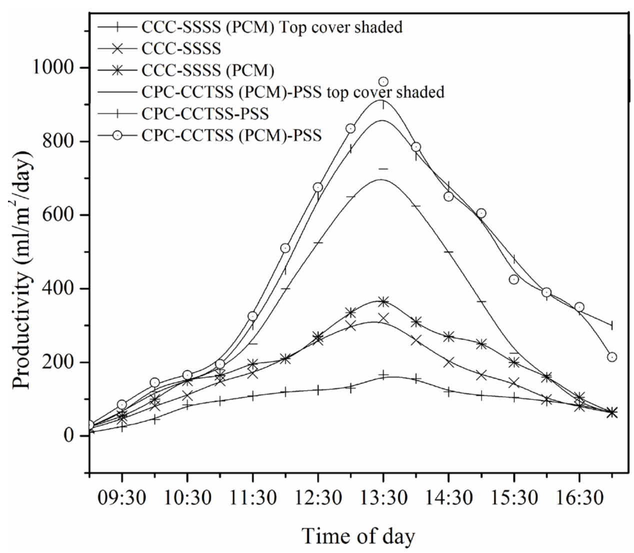

Fig. 24. Productivity with respect to system integration.

cover shaded were found as 2680 mL/m^2/d, 3240 mL/m^2/d, and 1646 mL/m^2/d, respectively. Similarly, the productivity of the CPC-CCTSS-PSS, CPC-CCTSS (PCM)-PSS and CPC-CCTSS (PCM)-PSS top cover shaded were found as 7160 mL/m^2/d, 7346 mL/m^2/d, and 5120 mL/m^2/d, respectively. The results clearly demonstrated that the top cover shaded solar still productivity does not drop to zero due the effect of system integration. The total productivity of the CPC-CCTSS (PCM)-PSS is high because the CPC-CCTSS itself acts as a solar still and delivers output. So the value of 7346 mL/m^2/d is the total productivity of CPC-CCTSS and PSS. After shading the PSS and SSSS, the combination of CPC-CCTSS and CCC-crescent shaped absorber act as primary heat delivery source to the distillers.

6. Conclusion

In this study, a CCC and CPC are coupled with SSSS and PSS. The concentrators are coupled to the solar stills. Therefore, the fresh water production is always available even when the SSSS and PSS top covers are blocked from sunlight. Two important mechanisms are used to supply the heat transfer; they are (1) thermosyphon effect in CCC-SSSS and (2) heat extraction technique in CPC-CCTSS-PSS. The results showed that the productivity of CCC-SSSS, CCC-SSSS with PCM and CCC-SSSS (PCM) top cover shaded were found as 2680 mL/m^2/d, 3240 mL/m^2/d, and 1646 mL/m^2/d, respectively. Similarly the productivity of the CPC-CCTSS-PSS, CPC-CCTSS (PCM)-PSS and CPC-CCTSS (PCM)-PSS top cover shaded were found as 7160 mL/m^2/d, 7346 mL/m^2/d, and 5120 mL/m^2/d, respectively. From the experimental evidence, it was found out that the productivity of the two distillers does not drop to zero even when the top covers are shaded. The concentrators are supplied the heat energy to enable continuous fresh water production. This study concludes that integration yields enhancement.

Acknowledgments

This study has received funding from Indian Ministry of New and Renewable Energy (MNRE). NREF/TU/2010/001 dated on 14.04.2010.

Symbols

A	—	Area
a	—	Perimeter
b	—	Radial gap
CR	—	Concentration ratio
D	—	Diameter
G	—	Gap thickness
I	—	Solar irradiance
K	—	Thermal conductivity
L	—	Length
R, r	—	Radius
r_1	—	Radius of receiver
r_2	—	Radius of envelope
PCM	—	Phase change material
CCC	—	Compound conical concentrator
CPC	—	Compound parabolic concentrator
SSSS	—	Single slope solar still
PSS	—	Pyramid solar still
CCTSS	—	Concentric circular tubular solar still

Greek symbols

α	—	Absorptance
δ	—	Gap thickness
ΔT	—	Difference in temperature
ε	—	Infra-red emissivity
η	—	Efficiency
μ	—	Viscosity
ρ	—	Ground reflectance
σ	—	Stefan Boltzmann constant
τ	—	Transmittance

References

[1] https://en.wikipedia.org/wiki/Tirukkural.
[2] K. Kalidasa Murugavel, S. Sivakumar, J. Riaz Ahamed, Kn.K.S.K. Chockalingam, K. Srithar, Single basin double slope solar still with minimum basin depth and energy storing material, Appl. Energ., 87 (2010) 514–523.
[3] A.A. Madani, G.M. Zaki, Yield of solar stills with porous basins, Appl. Energ., 52 (1995) 273–281.
[4] A.A. El-Sebaii, A.A. El-Naggar, Year round performance and cost analysis of a finned single basin solar still, Appl. Therm. Eng., 110 (2017) 787–794.
[5] S.O. Onyegegbu, Nocturnal distillation in basin-type solar stills, Appl. Energ., 24 (1986) 29–32.
[6] R. Bhardwaj, M.V. Ten Kortenaar, R.F. Mudde, Maximized productivity of water by increasing area of condensation surface for solar distillation, Appl. Energ., 154 (2015) 480–490.
[7] R. Segurado, J.F.A. Madeira, Costa M, Duic, M.G. Carvalho, Optimization of a wind powered desalination and pumped hydro storage system, Appl. Energ., 177 (2016) 487–499.
[8] Ashraf Elfasakhany, Performance assessment and productivity of simple-type solar still integrated with nano composites energy storage, Appl. Energ., 183 (2016) 399–407.
[9] Veera Gnaneswar Gude, Energy storage for desalination processes powered by renewable energy and waste heat sources, Appl. Energ., 137 (2015) 877–898.
[10] Rahul Dev, Sabah A. Abdul-Wahab, G.N. Tiwari, Performance study of the inverted absorber solar still with water depth and total dissolved solids, Appl. Energ., 88 (2011) 252–264.
[11] M.R. Karimi Estahbanati, Amimul Ahsan, Mehrzad Feilzadeh, Khosrow Jafapur, Seyedeh-Saba Ashrafmansouri, Mansoor Feilzadeh, Theoretical and experimental investigation on internal reflectors in a single-slope solar still, Appl. Energ., 165 (2016) 537–547.
[12] Guo Xie, Licheng Sun, Zhengyu Mo, Hongtao Liu, Min Du, Conceptual design and experimental investigation involving a modular desalination system composed, Appl. Energ., 179 (2016) 972–984.
[13] Shiva Gorjian, Barat Ghobadian, Teymour Tavakkoli Hashjin, Ahmad Banakar, Experimental performance evaluation of a stand-alone point-focus parabolic solar still, Desalination, 352 (2014) 1–17.
[14] Z.M. Omara, Mohamed A. Eltawil, Hybrid of solar dish concentrator, new boiler and simple solar collector for brackish water desalination, Desalination, 326 (2013) 62–78.
[15] T. Arunkumar, R. Jayaprakash, Amimul Ahsan, D.C. Denkenberger, M.S. Okundamiya, Effect of water and air flow on concentric tubular solar water desalting system, Appl. Energ., 103 (2013)109–115.
[16] Yih-Hang Chen, Yu-Wei Li, Hsuan Chang, Optimal design and control of solar driven air gap membrane distillation desalination systems, Appl. Energ., 100 (2012) 193–204.
[17] P.T. Tislingiris, The glazing temperature measurement in solar stills-Error and implications on performance evaluation, Appl. Energ., 88 (2011) 4936–4944.
[18] M.K. Gaur, G.N. Tiwari, Optimization of number of collectors for integrated PV/T hybrid active solar still, Appl. Energ., 87 (2010) 1763–1772.
[19] Shanmugapriya Balaji, K.S. Reddy, Sundararajan, Optical modelling and performance analysis of a solar LFR receiver system with parabolic and involute secondary reflectors, Appl. Energ., 179 (2016) 1138–1151.
[20] K. Ravi Kumar, K.S. Reddy, Thermal analysis of solar parabolic trough with porous disc receiver, Appl. Energ., 86 (2009) 1804–1812.
[21] K.S. Reddy, G. Veershetty, Viability analysis of solar parabolic dish stand-alone power plant for Indian conditions, Appl. Energ., 102 (2013) 908–922.
[22] Sendhil Kumar Natarajan, K.S. Reddy, Tapas Kumar Mallick, Heat loss characteristics of trapezoidal cavity receiver for solar liner concentrating system, Appl. Energ., 93 (2012) 523–531.
[23] Soteris Kalogirou, Use of parabolic trough solar energy collectors for sea-water desalination, Appl. Energ., 60 (1998) 65–78.
[24] D.C. Denkenberger, J.M. Pearce. Compound parabolic concentrators for solar water heat pasteurization: numerical simulation. Proceedings of the Solar Cookers International Conference in Granada, Spain, July 12–16, 2006.
[25] A.A. El-Sebaii, M. Al-Dossari, A mathematical model of single basin solar still with an external reflector, Desal. Water Treat., 26 (2011) 250–259.
[26] Hiroshi Tanaka, Optimum inclination of still and bottom reflector for tilted wick solar still with flat plate bottom reflector, Desal. Water Treat., 51 (2013) 6482–6489.
[27] Abdul Jabbar N. Khalifa, Hussein A. Ibrahim, Experimental study on the effect of internal and external reflectors on the performance of basin type solar stills at various seasons, Desal. Water Treat., 27 (2011) 313–318.
[28] B. Chaochi, A. Zrelli, S. Gabsi, Desalination of brackish water by means parabolic solar concentrator, Desalination 201 (2007) 118–126.
[29] T. Arunkumar, R. Jayaprakash, Amimul Ahsan, K. Vinothkumar, Effect of air flow on tubular solar still efficiency, Iranian J. Health. Sci. Eng., 10 (2013) 31.
[30] T. Arunkumar, R. Velraj, D.C. Denkenberger, Ravishankar Sathyamurthy, K. Vinothkumar, Amimul Ahsan, Effect of heat removal on tubular solar desalting system, Desalination, 379 (2016) 24–33.
[31] T. Arunkumar, R. Velraj, D.C. Denkenberger, Ravishankar Sathyamurthy, K. Vinothkumar, A. Ahsan, Productivity enhancements of compound parabolic concentrator tubular solar stills, Renew. Energ., 88 (2016) 391–340.
[32] T. Arunkumar, R. Velraj, D.C. Denkenberger, Ravishankar Sathyamurthy, Influence of crescent shaped absorber in water desalting system, Desalination, 398 (2016)208–213.
[33] T. Arunkumar, R. Velraj, Amimul Ahsan, A.J.N. Khalifa, S. Shams, D.C. Denkenberger, Ravishankar Sathyamurthy, Effect of parabolic solar energy collectors for water desalination, Desal. Water Treat., 57 (2016) 21234–21242.
[34] R.Z. Wang, T.S. Ge, Advances in solar heating and cooling. Woodhead publishing publications (Elsevier). 2016. ISBN: 978-0-08-100301-5.
[35] A.A. El-Sebaii, A.A. Al-Ghamdi, F.S. Al-Hazmi, A.S. Faidah, Thermal performance of a single basin solar still with PCM as a storage medium, Appl. Energ., 86 (2009) 1187–1195.
[36] Mona M. Naim, Mervat A. Abd El-Kawi, Non-conventional solar stills. Part 2. Non-conventional solar stills with energy element, Desalination, 153 (2002) 71–80.
[37] Abdulhaiy M. Radhwan, Transient performance of a stepped solar still with built-in latent heat thermal energy storage, Desalination, 171 (2004) 61–66.
[38] T. Arunkumar, D.C. Denkenberger, R. Velraj, R. Sathyamurthy, Hiroshi Tanaka, K. Vinothkumar, Experimental study on parabolic concentrator assisted solar desalting system, Energ. Convers. Manag., 105 (2015) 665–674.
[39] A.E. Kabeel, Mohamed Abdelgaied, M. Mohgoub, The performance of a modified solar still using hot air injection and PCM, Desalination, 379 (2016) 102–107.
[40] A.E. Kabeel, Mohamed Abdelgaid, Improving the performance of solar still by using PCM as a thermal storage medium under Egyptian conditions, Desalination, 383 (2016) 22–28.
[41] Mohammed Dashtban, Farshad Farshchi Tabrizi, Thermal analysis of a weir-type cascade solar still integrated with PCM storage, Desalination, 279 (2011) 415–422.
[42] Miqdam T. Chaichan, Hussein A. Kazem, Water solar distiller productivity enhancement using concentrating solar water heater and phase change material (PCM), Case Stud. Thermal Eng., 5 (2015) 151–159.
[43] Ravishankar Sathyamurthy, P.K. Nagarajan, J. Subramani, D. Vijayakumar, Mohammed Ashraj Ali, Effect of water mass on triangular pyramid solar still using phase change material as storage medium. Energy Procedia., 61 (2014) 2224–2228.
[44] T. Arunkumar, A.E. Kabeel, Effect of phase change material on concentric circular solar still: integration meets enhancement, Desalination, 414 (2017) 46–50.

[45] A.E. Kabeel, T. Arunkumar, D.C. Denkenberger, Ravishankar Sathyamurthy, Performance enhancement of solar still through efficient heat exchange mechanism- A review, Appl. Therm. Eng., 114 (2017) 815–836.
[46] T. Arunkumar, D. Denkenberger, Amimul Ahsan, R. Jayaprakash, The augmentation of distillate yield by using concentrator coupled solar still with phase change material, Desalination, 314 (2013) 189–192.
[47] T. Arunkumar, R. Jayaprakash, D. Denkenberger, Amimul Ahsan, M.S. Okundamiya, Sanjay kumar, Hiroshi Tanaka, H.Ş. Aybar, An experimental study on a hemispherical solar still, Desalination, 286 (2012) 342–348.
[48] Rachel Oommen. Development of compound parabolic solar concentrator with reduced gap losses application to steam generation. (Doctoral dissertation). Bharathiar University. http://hdl.handle.net/10603/101207, (1995).